17th Brazilian Congress of Thermal Sciences and Engineering
November 25th-28th, 2018, Águas de Lindóia, SP, Brazil

ENCIT-2018-0535
SOLAR INDUSTRIAL STEAM PRODUCTION TECHNOLOGIES: COMPARISON THROUGH MODELING, SIMULATION, AND ECONOMIC ASSESSMENT

Hendrius Oliveira
Universidade Federal de Itajubá, Av. BPS, 1303, Bairro Pinheirinho, Itajubá – MG
hendrius@unifei.edu.br

Prof. Dr. Osvaldo José Venturini
Universidade Federal de Itajubá, Av. BPS, 1303, Bairro Pinheirinho, Itajubá – MG
osvaldo@unifei.edu.br

Abstract. *The goal is to analyze and compare the three most common solar steam production technologies without thermal storage integrated into a conventional 1 MW steam production system through modeling, simulation and solar field size optimization through payback period and fuel saving by Direct Normal Irradiation (DNI), ambient temperature, and wind speed in two locations: one with high DNI, high temperature and low wind speeds and the other with lower DNI, lower temperatures and higher wind speed. The most economically viable system without thermal storage is the Direct Steam Generation system. However, higher operating temperatures make the use of systems that use water as a heat transfer fluid prohibitive. In these cases, the most suitable system, among those analyzed here, is the Unfired Boiler system. In addition, it is suggested that the advantages and disadvantages of each technology be considered according to the peculiarities of each case, such as safety and environmental risk issues. The factors that determine the feasibility of installing a solar thermal system are the fuel price, quantity of solar resource and the type of technology employed. However, fuel price and availability of solar resource are more relevant factors for economic viability than the type of technology employed.*

Keywords: *Solar thermal systems, Flash boiler system, Unfired boiler system, Direct Steam Generation system, Solar Industrial Process Heat.*

1. INTRODUCTION

Systems for generating steam with conventional fossil fuel boilers for industrial processes are common. However, the prices of these fuels are subject to variations influenced by several factors (Atalla *et al.*, 2017). However, as solar energy is a free and constantly available renewable resource, the integration of solar thermal systems for steam generation with conventional fossil fuel vapor generation systems for industrial processes can result in fuel savings and greater resistance to fossil fuel price variation (Kurup and Turchi, 2015).

The three most common types of solar systems for steam production are the Direct Steam Generation (DSG) system, where a two-phase flow is allowed in the collector directly generating steam, the Flash Boiler (FB) system, in which pressurized water liquid flow in the collector to be expanded later in a separate vessel, and the Unfired Boiler (UB) system in which the Heat Transfer Fluid (HTF) is circulated in the collector and vapor is generated indirectly, on the heat exchanger (Kalogirou, 2014).

Most industrial process heat applications require operating temperatures below 200 °C (Sharma *et al.*, 2017). Also, a 1 MW size industrial steam production system is common.

To make the optimum economic decision it is necessary to know, based on the economic indicator of interest, the optimal solar field dimension of the solar thermal system to be integrated into the conventional steam system. The cost of the solar thermal system is composed of costs involving collectors, control system, piping, HTF, tracking system, heat exchanger and others. The economic indicator chosen to optimize the size of the solar thermal systems in this work is the payback period.

The constraints that allow the solar field size optimization are the fixed steam demand required by the system and the low efficiency of the conventional system of steam generation at low partial loads. As industrial processes usually have a constant vapor demand (Kalogirou, 2014), an oversized solar field causes large energy waste at times of high solar irradiance for solar systems without thermal storage. In addition, another limiting factor is that conventional steam generation systems generally lose efficiency for low steam demands, below 30% of nominal capacity (Bujak, 2008).

The main parameters that could influence the energy and economic index are Direct Normal Irradiation (DNI), ambient temperature, wind speed, and fuel price. Because those characteristics vary with location, it is interesting to

analyze the economic index on two different regions. Meteorological measurements from Brasilia (Brazil) and Edmonton (Canada) can be obtained from NREL (2017) available in 30 minutes intervals, proper to steady-state analyses. Brasilia and Edmonton climates are practically opposites, the former has high DNI and temperature levels and low wind speed levels, the latter has lower DNI and temperatures and higher wind speeds.

Therefore, the goal is to analyze and compare, through modeling, simulation and solar field size optimization based on the payback period and fuel saving, the three most common solar generation technologies without thermal storage (UB, FB and DSG systems) integrated into a conventional 1 MW steam production system that delivers steam at 200°C, considering measurements between 30 minute intervals of DNI, ambient temperature, wind speed and fuel price in two strategically distinct locations: one with high DNI, high temperature and low wind speeds (Brasília, Brazil) and the other with lower DNI , lower temperatures and higher wind speeds (Edmonton, Canada). It is expected to obtain the energy performance and economic viability of each technology of steam generation analyzed together with literature to evaluate the advantages and disadvantages of each technology and how the economic viability depends upon meteorological parameters, solar resource, fuel price and type of technology employed.

2. METHODOLOGY

2.1. Systems general description

The parabolic trough collector considered here is the model S10 of the company Rackam. Its main parameters are set out in Tab. 1. The collectors are installed with an axis parallel to the earth axis of rotation (north-south polar axis) so that the tracking system rotates during the day in the east-west direction in order to intercept as much DNI as possible. This orientation set up has the advantage of having the most balanced performance between the seasons of the year compared to others single-axis tracking configurations (Kalogirou, 2014).

Table 1. Rackam parabolic trough collector parameters.

Parameters	Value	Source
Collector length	24,38 m	Rackam (2018)
Collector width	1,16 m	Rackam (2018)
Glass envelop outside diameter	0,065 m	Rackam (2018)
Glass envelop inside diameter	0,060 m	Estimated
Absorber pipe outside diameter	0,0318 m	Rackam (2018)
Absorber pipe inside diameter	0,0278 m	Rackam (2018)
Intercept factor	0,89	Estimated based on Fernadez-Garcia *et al.* (2010)
Glass envelope transmittance	0,95	Estimated based on Fernadez-Garcia *et al*. (2010)
Glass envelope absorptance	0,02	Kalogirou (2012)
Absorber pipe absorptance	0,96	Dudley *et al.* (1994)
Reflectance of the clean mirror	0,89	Estimated based on Fernadez-Garcia *et al*. (2010)
Factor due dirt on mirror	0,989	Duffie *et al.* (1991)
Factor due dirt on absorber pipe	0,994	Duffie *et al.* (1991)
Glass envelope emittance	0,86	Kalogirou (2012)
Glass thermal conductivity	1,04 W/(m°C)	Kalogirou (2012)
Absorber pipe emittance	0,06 (100°C) to 0,15 (400°C)	Kalogirou (2012)
Absorber pipe material type	Stainless steel 304L	Kalogirou (2012)
Vacuum annulus pressure	< 0,013 Pa	Dudley *et al*. (1994), Kalogirou (2012)
Maximum operating temperature	240 °C	Rackam (2018)

Steam in a UB system is produced in the evaporator by receiving heat from the main circuit, which in this case is composed of the mineral oil that circulates through the parabolic trough collectors (Fig. 1). In the collectors, part of the DNI is absorbed as oil sensitive heat due to being concentrated on the receiver by the parabolic reflector and the other part is lost. The oil pump is used to control the maximum system temperature (in this case, 240 ° C) by varying the mass flow rate of oil in the collectors. In the heat exchanger, a bundle of tubes through which hot oil circulates yields heat to the liquid saturated water that undergoes a pool boiling evaporation process. Then, cold oil (~ 210 ° C) recirculates in the collectors and saturated steam at 200 ° C is finally produced, which will integrate the pre-existing conventional steam production system circuit. The controlling can be done by measuring the HTF temperature in the hot oil piping section and, then, varying the oil pump mass flow rate through a correctly calibrated feedback loop.

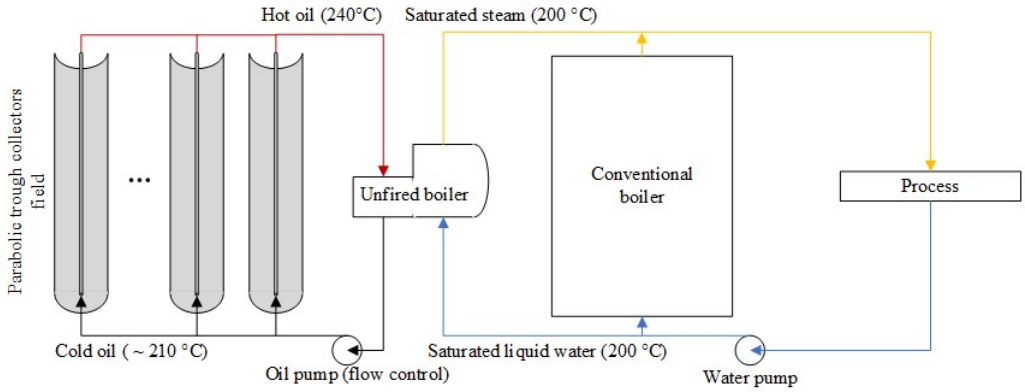

Figure 1. UB system and conventional system integrated.

In the FB system, shown in Fig. 2, water is the HTF. The collector receives subcooled liquid water at 200 ° C and operates so that 220 °C saturated water is produced at the collector outlet. Similar to the UB system, the flow is controlled by the pump through speed control methods in order to regulate the temperature at the collector output to a constant value of 220 °C. In this system, the steam is produced in the expansion valve where the water is adiabatically expanded to the flash tank pressure, which equals the conventional system steam pressure (Fig. 2).

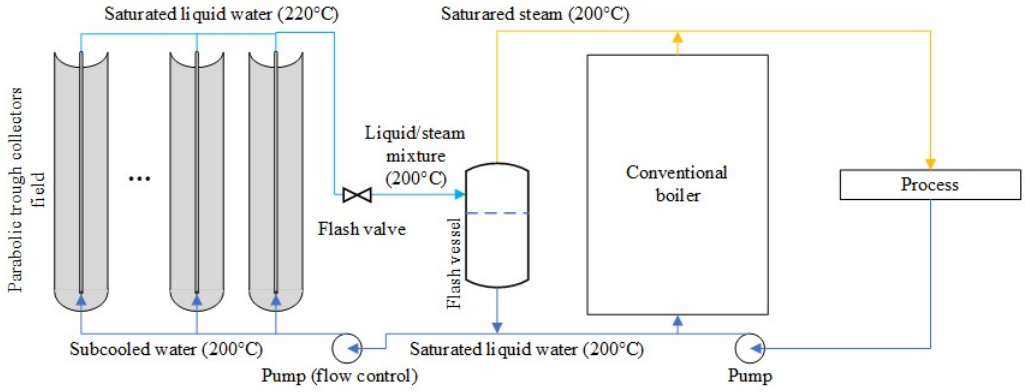

Figure 2. FB system and conventional system integrated.

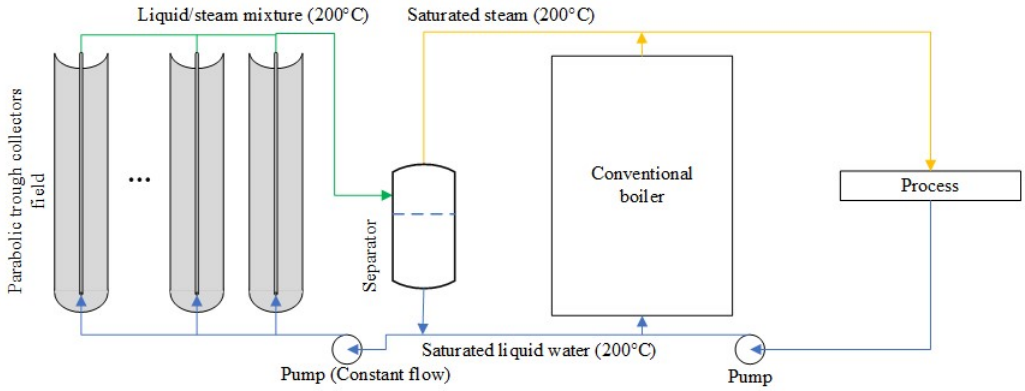

Figure 3. DSG system and conventional system integrated.

In the DSG system, there is no HTF temperature gradient, which in this case is also water. In this system, solar energy absorbed by the collector is stored in the water as latent heat, that is, steam is produced directly as the water receives heat. Thus, at the collector outlet, when in operation, the water is in a wet vapor state with quality less than 16% (design value). After reaching the separator tank, the steam generated is added to the conventional system steam circuit and the saturated liquid is recirculated to the collectors (Fig 3). Another difference of this system compared to the others is that, for this system, the HTF mass flow rate inside the collectors is constant (in this case, 0.0607 kg/s),

being the collectors steam quality output a value that depends upon the DNI value. This configuration makes the control simpler compared to other systems that require speed control methods at the pump.

2.2. Study Strategy

Firstly, the integrated solar systems were modeled accordingly to the available literature. The model of each solar thermal system was used to analyze the relationship between energy performance parameters (overall efficiency and thermal loss) and meteorological parameters (DNI, ambient temperature, and wind velocity) in order to evaluate the parameters relevance for the energy performance.

Secondly, DNI, ambient temperature and wind speed at 30 minutes intervals data from NREL (2017) of two strategically distinct locations (one with more favorable meteorological conditions than the other) during the year 2014 were simulated in the proposed models of each solar thermal system. The proposed models take into account only a single solar collector first; afterward, these results are extrapolated for an optimal number of solar collectors. The results obtained from this simulation were: the relationship between the steam flows produced by each solar thermal system with meteorological input parameters at each measurement point during the year 2014 at the two locations considered.

After the solar thermal systems simulation at all measurement points on the locations, the vapor mass flow produced for each measurement point was used this time as input data, together with fuel price, for solar field size optimization and payback period calculation considering the conventional system operating model.

Finally, the final results of energy and economic performance are analyzed together with available literature bibliography in order to compare the solar technologies here pointed out and evaluate the relevance of meteorological, technological and location parameters for economic feasibility.

2.3. Modeling

All models proposed in this study are based on a steady state analysis. Also, all solar thermal systems are modeled accordingly to energy balances in specific collector components. The Fig. 4 shows the cross-section of the receiver, which includes the glass envelope, the absorber pipe, the HTF and the vacuum annulus space between glass and pipe, and the energy flux dynamic between the collector receiver components. The inside surface of the absorber pipe has the subscript *pi* and its outside surface has the subscript *po*, the inside of the glass envelope has the subscript *gi* and its outside has the subscript *go*, the HTF is represented through the subscript *f* and the air and sky are represented by the subscripts *a* and *s*, respectively. The solar DNI hits the receiver after being focused by the collector reflective surface. Part of this solar energy is absorbed by the absorber pipe outside surface, $Q_{po,SolAbs}$ (W) after a previous minor part is absorbed by the glass envelope outside surface, $Q_{go,SolAbs}$ (W). Then, part of $Q_{po,SolAbs}$ is transferred through the pipe until the inner side by conduction, $Q_{pi-p\ ,cond}$ (W), and afterward transferred to the HTF by convection, $Q_{f-pi,conv}$ (W). The other part of $Q_{po,SolAbs}$ is lost through convection, $Q_{po-g\ ,conv}$ (W), and radiation, $Q_{po-g\ ,rad}$ (W), to the glass envelope inside surface. Finally, the heat received by the glass inner surface is transferred through the glass to its outside surface by conduction, $Q_{gi-go,cond}$ (W), where $Q_{go,SolAbs}$ is added to the transferring heat and then all is lost to the environment by convection, $Q_{go-a,conv}$ (W), and to the sky by radiation, $Q_{go-s,rad}$ (W). All heat transfer calculations are detailed in Kalogirou (2012), with exception of the DSG system $Q_{f-pi,conv}$, that it is calculated accordingly to two-phase flow theory. That is, the flow pattern map and boiling crisis analysis are done accordingly to Thome and Hajal (2003) and the heat transfer calculation accordingly to Kind and Saito (2010).

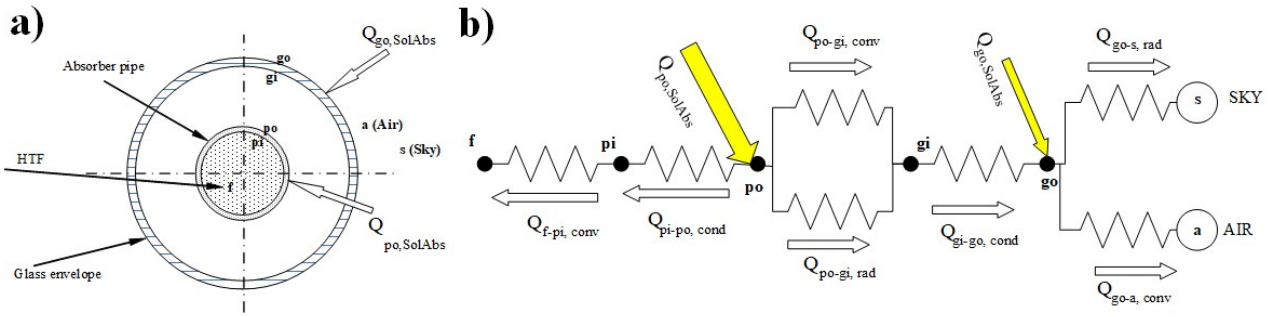

Figure 4. a) Solar collector receiver cross-section. b) Heat transfer through receiver components.

The main goal of all solar thermal systems models is to calculate the steam mass flow rate produced in kg/s, $\dot{m}_v$, accordingly to Eq. (1), the thermal loss in W/m², Q_{loss}/A_{col}, accordingly to Eq. (2), and the solar-to-steam energy efficiency, η_{sol}, accordingly to Eq. (3).

$$\dot{m}_v = Q_{f-pi,conv}/\Delta H_{LG} \tag{1}$$

$$Q_{loss}/A_{col} = \left(Q_{go-a,conv} + Q_{go-s,rad} - Q_{go,SolAbs}\right)/A_{col} \quad (2)$$

$$\eta_{sol} = Q_{f-pi,conv}/(DNI \cdot A_{col}) \quad (3)$$

The term ΔH_{LG} is the heat of vaporization of water at 200°C and A_{col} is net collector aperture area in m².

All parameters necessary to calculate the steam mass flow, thermal loss, and overall efficiency are obtained by solving nonlinear equations systems. The non-linear equations systems consist of equations from energy and mass balances on the receiver and solar system components. Moreover, all nonlinear equations systems present in this paper were solved based on the method proposed by Xiao and Yin (2017).

The UB system nonlinear equations consist of the energy balance on the HTF control volume, considering the heat transfer in a cross-section direction, detailed in Eq. (4), the energy balance on the absorber pipe, detailed in Eq. (5), the energy balance on the vacuum annulus, detailed in Eq. (6), the energy balance on the glass envelope, in Eq. (7), the longitudinal mass and energy balance on the HTF, detailed in Eq. (8), that is, considering the difference between the HTF inlet temperature, T_{fi}, and outlet temperature, T_{fo}, of which Q_{fi-fo} is the heat gained by the HTF. The last equation which integrates the UB nonlinear system is the energy and mass balance on the UB heat exchanger, shown in Eq. (9), in which $Q_{f-w,pool}$ is calculated accordingly to the steady state model validated by Bonilla *et al*. (2017) and considering that the type of convective heat transfer process in the heat exchanger is the pool boiling type, calculated accordingly to Gorenflo and Kenning (2009). The independent variables in the UB nonlinear equations are the inside and outside absorber pipe temperatures, the inside and outside glass envelope temperatures, the HTF mass flow rate, and the HTF inlet temperature, closing the 6 linear independent variables necessary to solve the system.

$$0 = Q_{f-pi,conv} - Q_{pi-po,cond} \quad (4)$$

$$0 = Q_{po,SolAbs} - Q_{po-gi,conv} - Q_{po-gi,rad} - Q_{pi-po,cond} \quad (5)$$

$$0 = Q_{po-gi,conv} + Q_{po-gi,rad} - Q_{gi-go,cond} \quad (6)$$

$$0 = Q_{go,SolAbs} + Q_{gi-go,cond} - Q_{go-s,rad} - Q_{go-a,conv} \quad (7)$$

$$0 = Q_{fi-fo} - Q_{f-pi,conv} \quad (8)$$

$$0 = Q_{f-w,pool} - Q_{fi-fo} \quad (9)$$

The FB system nonlinear equations are similar to the UB system. The differences are that the FB system has no heat exchanger and the HTF is now water. Therefore, its nonlinear equations are Eq. (4), (5), (6), (7) and (8). Also, the inlet temperature is subtracted from the independent variables list and the remaining 5 linear independent variables close the nonlinear system solution.

Because the DSG system control is different, that is, the HTF mass flow is constant and there is no HTF temperature gradient along the collector, its nonlinear equations consist of Eq. (4), (5), (6) and (7) plus Eq. (10) below, in which A_{pi}, m², is the inner surface of the absorber pipe. Also, as the water mass flow rate is constant, the heat flux, $\dot{q}$ (W/m²), take its place as an independent variable for solving the nonlinear system. As result, the independent variables in the UB nonlinear equations are the inside and outside absorber pipe temperatures, the inside and outside glass envelope temperatures and the heat flux, closing the 5 linear independent variables necessary to solve the system.

$$0 = \dot{q}A_{pi} - \left\{Q_{po,SolAbs} - \left[Q_{go-a,conv} + Q_{go-s,rad} - Q_{go,SolAbs}\right]\right\} \quad (10)$$

The main component of a conventional steam production system is the boiler. In the boiler operation performance modeling, detailed in Eq. (11), in which η_{boiler} is the boiler fuel-to-steam overall efficiency, it is assumed that the boiler has an energy loss fraction proportional to the flue gas mass flow, ϱ_{stack} with value 0,25, and other loss fraction associated with the heat lost to the environment by convection and radiation on the boiler skin, ϱ_{skin} assumed constant here with value 0,015, as proposed by Kutscher *et al*. (1983). As shown in Eq. (11), the boiler efficiency varies with the firing rate, F, which is the fraction of steam heat delivered to the process by the boiler relative to the boiler nominal power, $Q_{nominal}$ with a value of 1 MW in this case. Now, the firing rate is directly associated with the instantaneous process load required, in this cases is assumed a constant process load equivalent to the boiler nominal power, and the

instantaneous solar energy steam input produced by the solar thermal system, $Q_{v,sol,i}$ (W), determined by Eq. (13), in which N_{col} is number of collectors, and $\dot{m}_{v,i}$ is the steam mass flow calculated by Eq. (1) for the specific input data set. However, because the boiler efficiency decays sharply to zero when the firing rate is close to zero, it is assumed that the boiler operates in the $0 \leq F \leq 5\%$ range with a constant value of F = 5%. So, there are only 3 boiler operation scenarios: the boiler is off when $Q_{v,sol,i} \geq Q_{nominal}$ and boiler overall efficiency has no meaning in this case; the boiler operates with $F = 5\%$ when $0{,}95Q_{nominal} < Q_{v,sol,i} < Q_{nominal}$ and the boiler overall efficiency if given by Eq. (14), resulting in the loss of all solar energy steam input; and, finally, the boiler operates accordingly to Eq. (15), because $0 \leq Q_{v,sol,i} \leq 0{,}95Q_{nominal}$.

$$\eta_{boiler} = \frac{1}{1 + \varrho_{stack} + \frac{\varrho_{skin}}{F}} \tag{12}$$

$$Q_{v,sol,i} = N_{col}\dot{m}_{v,i}\Delta H_{LG} \tag{13}$$

$$F = \frac{Q_{nominal} - 0{,}95Q_{nominal}}{Q_{nominal}} \tag{14}$$

$$F = \frac{Q_{nominal} - Q_{v,sol,i}}{Q_{nominal}} \tag{15}$$

The economic index chosen is the payback period, t_{PB} (years), detailed in Eq. (16), in which C_{sol} is the total solar thermal system cost in US$ and $Y_{savings}$ is annual fuel saving return in US$/year. The annual fuel saving return is calculated accordingly to Eq. (17), in which c_{fuel} is the variable fuel price in US$/GJ that vary across time and location and $E_{savings}$ is the total year fuel energy savings in J/year calculated through Eq. (18), that considers the sum of energy savings in each data point interval, $E_{savings,i}$, throughout the year. However, $E_{savings,i}$ depends on the boiler operation: if $Q_{v,sol,i} \geq Q_{nominal}$ then $E_{savings,i}$ is calculated by Eq. (19), in which Δt is the time interval between data point, equals 1600s in this case; if $0{,}95Q_{nominal} < Q_{v,sol,i} < Q_{nominal}$ then $E_{savings,i}$ is calculated accordingly to Eq. (20); finally, if $0 \leq Q_{v,sol,i} \leq 0{,}95Q_{nomin}$ then Eq. (21) is used to calculate $E_{savings,i}$. Lastly, C_{sol} is calculated by Eq. (22), in which C_{HTF} is the total HTF cost in US$, C_{col} is total collectors cost in US$ and term on the right, that multiplies those parameters, is a scale factor proposed by Kutscher *et al*. (1983). The cost C_{col} is calculated based on the specific collector price suggested by Kurup and Turchi (2015) of 200 US$/m². Because Murphy and May (1982) estimated that FB system collector costs about 5% more than the DSG system due to greater pumping power requirement and operation pressure issues, we choose the specific collector cost of 200 US$ for the DSG system and 210 US$ for the FB and UB system. However, considering that HTF costs are different between the UB and FB system, C_{HTF} were calculated accordingly to mineral oil and water prices given by Kurup and Turchi (2015).

$$t_{PB} = C_{sol}/Y_{savings} \tag{16}$$

$$Y_{savings} = c_{fuel}E_{savings} \cdot 10^{-9} \tag{17}$$

$$E_{savings} = \sum_{i=1}^{N} E_{savings,i} \tag{18}$$

$$E_{savings,i} = E_{nominal}\Delta t \tag{19}$$

$$E_{savings,i} = \frac{(Q_{nominal} - 0{,}95Q_{nominal})}{\eta_{boiler}}\Delta t \tag{20}$$

$$E_{savings,i} = \frac{(Q_{nominal} - Q_{v,sol,i})}{\eta_{boiler}}\Delta t \tag{21}$$

$$C_{sol} = (C_{HTF} + C_{col})[-0{,}19\, ln(A_{col}N_{col}) + 2{,}202] \tag{22}$$

2.4 Operation conditions and simulation logic

The nonlinear equations systems are solved accordingly to Kind and Saito (2010). However, the method only works if $Q_{f-pi,conv}$ is greater than Q_{loss}. Otherwise, the HTF would cool down and never reach the outlet temperature of 240°C to the UB system and 220°C to the FB system. Thus, before solving the nonlinear equations, the thermal loss needs to be estimated then, based on the estimated thermal loss value, $Q_{loss,est}$, it is decided whether the solar system operates or doesn't operate (called stall mode). The estimated thermal loss is calculated by Eq. (22), in which U_{loss} the global heat transfer coefficient in W/m²/K calculated based on the estimated temperatures, A_r is the absorber pipe external surface area in m², $T_{po,est}$ is the estimated outside absorber pipe temperature and T_a is ambient temperature. For the $Q_{loss,est}$ estimation, it is considered that HTF and inlet absorber pipe temperatures are equal to $T_{po,est}$ and the inlet and outlet glass envelope temperatures are equal to T_a.

$$Q_{loss,est} = U_{loss} A_r (T_{po,est} - T_a) \tag{22}$$

For the energy performance analysis, only the solar systems are simulated to a range of DNI, ambient temperature and wind velocity following the Fig. 5 flowchart. In this analysis, the simulation considers only one collector and no optimization is done. Now, for the economic analysis, the NREL (2017) data from Brasilia and Edmonton are used to simulate the performance of one collector throughout the whole year data points following the Fig. 6 step-by-step processes. Afterward, the stored data from the previous simulation are analyzed considering the boiler model and the economic analysis accordingly to the Fig. 7 flowchart, extrapolating the single collector performance to optimize the solar field.

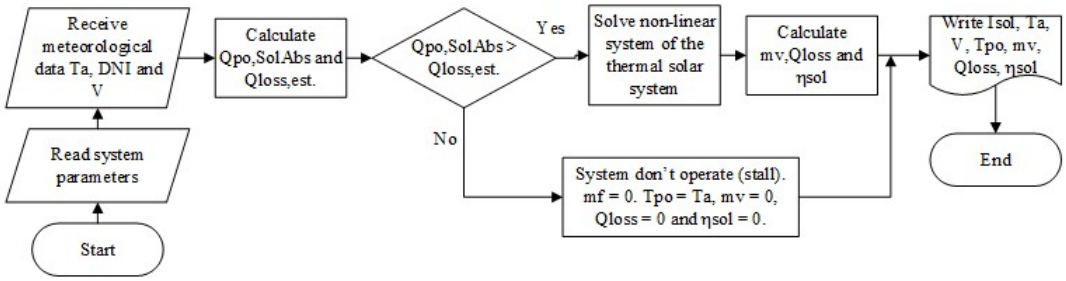

Figure 5. Flowchart used for solar thermal systems energy performance analysis.

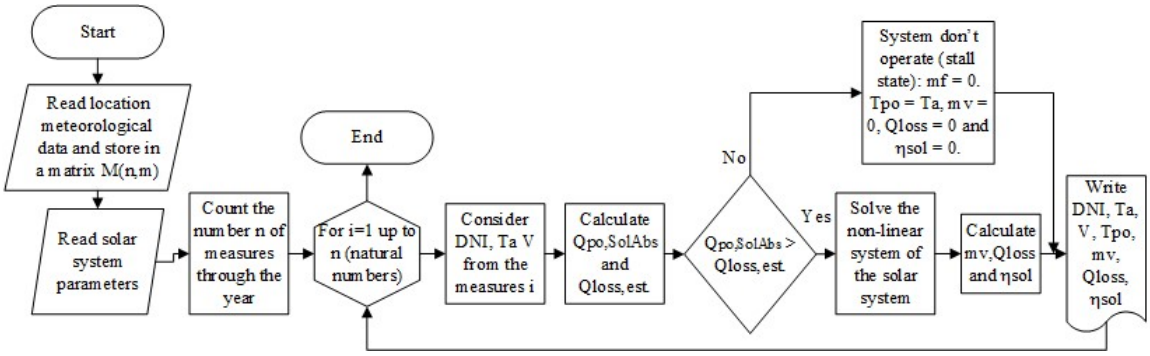

Figure 6. Flowchart used for solar thermal system simulation considering specific location data.

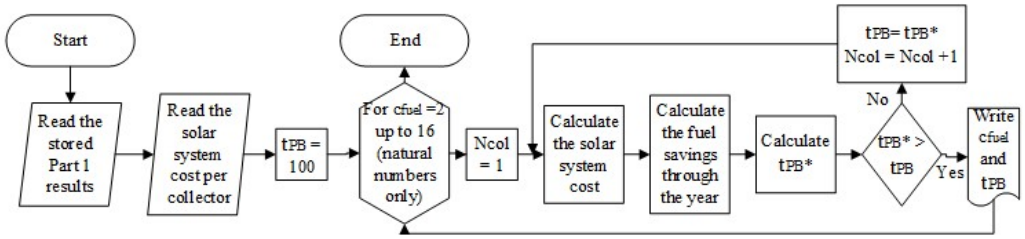

Figure 7. Flowchart of solar field size optimizing and economic analysis.

3. RESULTS

The overall efficiency drops sharply to zero as the value of energy that enters the system approaches the value of the thermal losses to the environment (which remains approximately constant), at which point all incoming energy is totally equivalent to losses (Fig. 8).

The mean absorber pipe temperature increases with DNI. Besides that, the thermal loss is directly correlated with the mean absorber pipe temperature, as can be seen on the shape similarity between the thermal loss and absorber pipe temperature curves, most visible on UB system (Fig. 9), which agrees with Eq. 22. The system with higher, medium and lower mean absorber pipe temperature are the UB, FB, and DSG, respectively.

The thermal loss of all solar thermal systems slightly decreases with ambient temperature. However, even within a wide range of ambient temperature variation, the thermal loss variation is small, since the overall efficiency is practically unchanged, which allows a reasonable approximation of the loss as being independent of ambient temperature (Fig. 10).

The systems with better, medium and worst overall efficiency and thermal loss are DSG, FB, and UB respectively (Fig. 8, 9 and 10).

The UB system has the greater payback period. This happens because this system is the most expensive of the systems, due to the greater complexity of the control system and due to the higher price of the HTF, in this case, the mineral oil. In addition, the UB system has the lowest efficiency among the three systems. These combined characteristics result in the greatest payback period. The FB system has the payback in an intermediate position when compared to the other systems. Its cost, excluding the cost of the HTF, is the same as the UB system because the control is also complex and the required pump pressure is the highest. The cost of the DSG system is the smallest due to the relatively simple control compared to the other systems and because its HTF is water that operates at a pressure lower than the FB system HTF operating pressure. In addition, its efficiency is the largest among systems. The combination of these features means that the DSG system has the lowest payback period compared to the other systems (Fig. 11).

In addition, the solar resource related to the system location has a greater effect on the viability of the project than the type of technology chosen. It is possible to note this in Fig. 11, where the curves of the technologies for the same location are much closer to each other, compared to their distance from the curves of the other location that are farther away. Edmonton's lower DNI values increase the payback period of all technologies in relation to payback periods in Brasilia more intensely than the increase in payback period caused due to technologies differences.

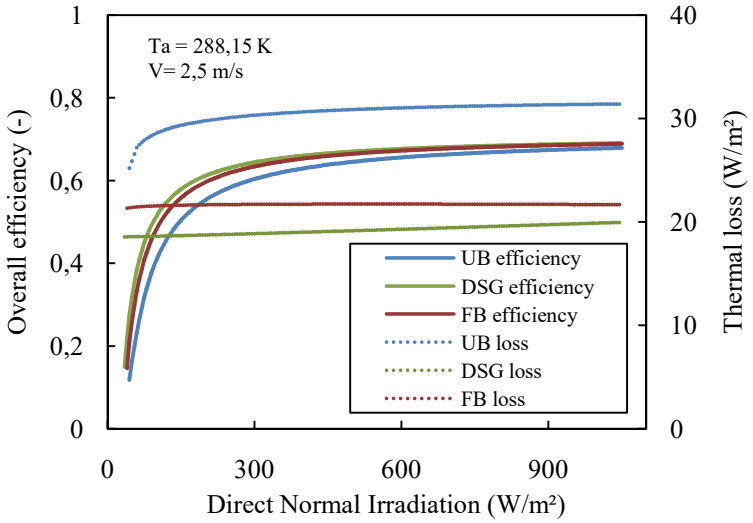

Figure 8. DNI influence on energy performance.

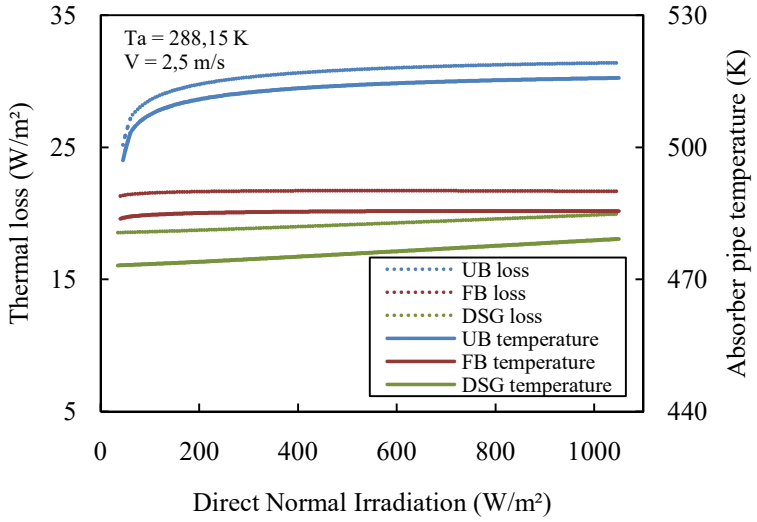

Figure 9. The relationship between absorber pipe temperature, thermal loss, and DNI.

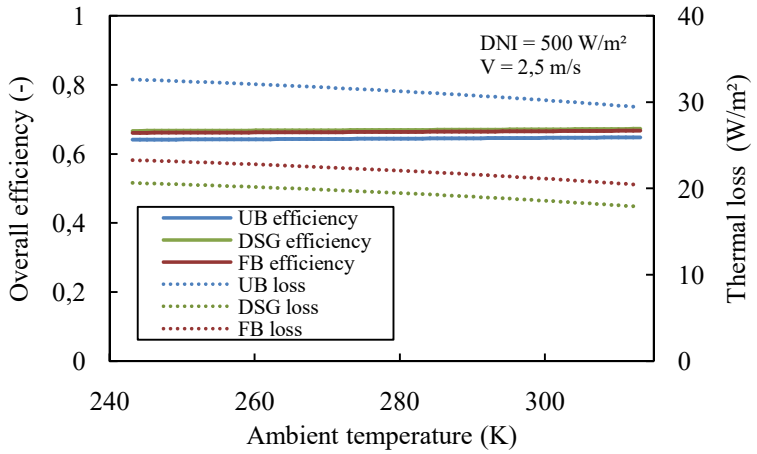

Figure 10. Ambient temperature influence on energy performance.

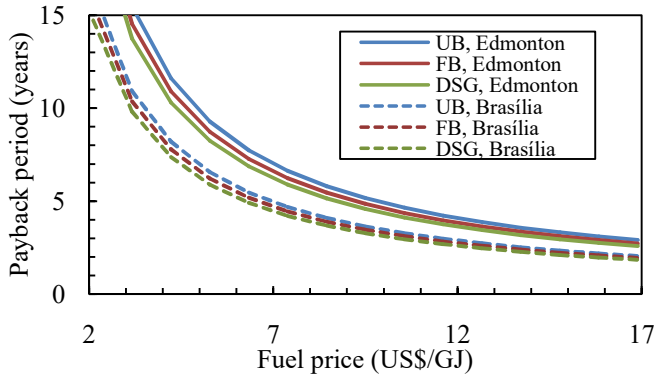

Figure 11. Economic feasibility of the solar system considering fuel price and location.

Considering a DNI of 500 W/m², an ambient temperature of 288,15 K and a wind velocity increase of 0 to 15 m/s, the thermal loss increases 0,645 W/m², 0,386 W/m² and 0,316 W/m² for the systems UB, FB, and DSG, respectively. In addition, considering the same conditions, the global efficiency decreases 0,14%, 0,08% and 0,07% for the systems UB, FB and DSG, respectively. Therefore, the energy performance is practically independent of wind velocity.

The mean HTF temperature inside the absorber pipe is close to 225 °C, 210 °C and 200 °C for the UB, FB and DSG systems, respectively. The UB and FB systems mean HTF temperatures are higher due to the temperature gradient formed upon the sensible heat transfer process compared to the constant DSG system HTF temperature of the latent heat transfer process. The difference between the mean HTF temperature and mean absorber pipe temperature range

between 0,25°C and 6°C, for the FB and DSG systems, and between 10°C to 20°C, for the UB system. Those temperature differences differ a lot because the mineral oil on the UB system has much worse heat transfer properties compared to the water on the FB and DSG system.

4. DISCUSSION

The modeling of the FB system and the parabolic trough collector in the UB system is based on the Kalogirou (2012) model. Although, more equations were added in order to account for the temperature control, in other words, because the mass flow is now a variable. The Kalogirou (2012) proposed method was already validated by him using data by Dudley (1994).

The modeling of the UB system is based on the integration of the parabolic trough collector with the unfired boiler (heat exchanger). The parabolic trough collector part uses the already validated Kalogirou (2012) model and the unfired boiler uses the steady state model presented by Bonilla *et al.* (2017). Although, as the output temperature of the collector is controlled by varying the mass flow, one more equation was added to solve the nonlinear system.

Finally, the modeling of the DSG system was not validated through experimental data. However, the models' results were compared with the results from Murphy and May (1982) and the results coherence indicated consistency.

The UB system has the worst energy performance. That is due to the inferior heat transfer properties of the mineral oil compared to the water and the temperature gradient on the absorber tube. These factors cause a greater mean absorber tube temperature, hence rising the thermal loss accordingly and, consequently, lowering the overall efficiency. Also, the UB system has the worst financial index. This system has the highest cost due to its complex control system and higher mineral oil cost in comparison to the cost of water. That allied to the inferior overall efficiency results in the worst financial decision from a purely economic standpoint. However, there are other factors involving the UB system besides the energy performance and economical index aspects. That is, the fact that oils are flammable, have environmental contamination hazard and are generally avoided in the foods and beverages industry due to product contamination hazard too (Murphy and May, 1982). Moreover, even though mineral oil is cheaper than synthetic oils, it has extremely high viscosity values at low temperatures, a factor that leads to the necessity of displacement pumps or some fluid heating device to start the fluid flow at low ambient temperatures, which would result in additional costs (Kurup and Turchi, 2015). Besides that, the UB system has some unique advantages. It is the most appropriate technology for high temperature saturated steam production applications because the water needs extremely high pressures to deliver high temperature saturated steam what makes the FB and DSG systems unsuitable for these applications (Häberle, 2012). Other benefits are not HTF freezing, non-corrosivity and low operating pressure (Kalogirou, 2014). Moreover, although the thermal storage technology, which can be used in UB system, was not considered in this study, Powell and Edgar (2012) concluded that the system overall stability could be improved through this technology due to the fact that solar energy is stored to be used flexibly. Furthermore, even the overall efficiency could be increased with thermal storage by using control techniques (Powell *et al.*, 2014).

The FB system has intermediary energy performance. Its HTF characteristics are better compared to the UB system mineral oil heat transfer characteristics. That is, the water good heat transfer characteristics lower the temperature difference between the absorber pipe and the water and consequently the absorber pipe outside temperature, which results in lower thermal loss to the environment. Also, the FB system has an intermediary financial index. Its cost is intermediary compared to the other systems. The system equipment and controls costs are the same compared to the UB system but its HTF cost is cheaper. Compared to the DSG system, the FB system has higher costs due to simple control used and lower pump power required in the operation of the DSG system. Hence, the FB system has the energy performance and cost intermediary, which results in an intermediary financial index. Along with the complex control required, the freezing issue of the water at low temperatures is another disadvantage. This issue forces the installation of heating and control devices that protect the system against water freezing (Murphy and May, 1982).

The DSG system has the same advantages and disadvantages that accompany the use of water as HTF. However, this system has the added advantage of operating at lower HTF temperature, which results in improved energy performance. In addition, another advantage is that the control of this system is simple (on and off). The water and the simple control have lower costs, which combined with improved energy performance results in the best economic index of all three technologies.

Therefore, the most economically viable system without thermal storage is the DSG system. However, higher operating temperatures make prohibitive the use of systems that use water as an HTF. In these cases, the most suitable system, among those analyzed here, is the UB system. In addition, it is suggested that the advantages and disadvantages of each technology be considered according to the peculiarities of each case. Others dimensions of analysis must be taken into account for the selection of a technology beyond the economic dimension, such as safety and environmental risk.

Although the external temperature of the absorber, which is directly related to the thermal loss, is a function of the DNI, its dependence is only apparent for values where the efficiency of the system is close to zero, because of that this dependency can be rejected. Moreover, the thermal loss also practically does not vary with wind velocities due to the insulation of the glass envelope and the evacuated space between the tubes, as was also investigated by Dudley *et al.* (1994). Also, the dependence of the thermal loss as a function of the ambient temperature is small over a wide range of ambient temperatures, because of that considering the loss as constant relative to the ambient temperature is a

reasonable approximation. Thus, it can be extrapolated that the meteorological parameters have little influence on the economic viability of the system, being the amount of net solar energy available to be absorbed during the year much more relevant. In addition, the variation of the payback period as a function of fuel price is significant. The greater influence of the fuel price compared to the type of technology chosen can be practically observed by considering the current price of natural gas in Brazil of approximately 10 US$/GJ (COPERGAS, 2018) and the average price of natural gas in Canada of approximately 2.7 US$/GJ (NATURAL RESOURCES CANADA, 2018). That is, considering payback period below 5 years economic attractive, all considered technologies are viable in Brasilia and yet with little differences in payback period. However, for the price of natural gas in Canada, no technology would be viable in Edmonton. That indicates that the fuel price is much more relevant for the economic feasibility than the technology type chosen.

Therefore, the factors that determine the project economic feasibility of installing a solar thermal system to be integrated into a conventional steam generation system are the conventional system fuel price, solar resource and type of technology employed. However, fuel price and availability of solar resource are more relevant factors for economic viability than the type of technology employed.

5. ACKNOWLEDGMENTS

The authors acknowledge the financial support of the Fundação de Amparo à Pesquisa do Estado de Minas Gerais (FAPEMIG) and the Conselho Nacional de Pesquisa e Desenvolvimento Científico e Tecnológico (CNPq).

6. REFERENCES

Atalla, T., Blazquez, J., Hunt, L.C. and Manzano, B. “Prices versus policy: An analysis of the drivers of the primary fossil fuel mix”. *Energy Policy*, Vol. 106, p. 536–546, 2017.

Bonilla, J., Calle, A., Rodríguez_García, M. M., Roca, L. and Valenzuela, L.*”* Study on shell-and-tube heat exchanger models with different degree of complexity for process simulation and control design”. *Applied Thermal Engineering*, Vol. 124, p. 1425–1440, 2017.

Bujak, J. “Mathematical modelling of a steam boiler room to research thermal efficiency”. Energy, Vol. 33, p. 1779–1787, 2008.

COPERGAS. “Tarifas”. 27 mar. 2018. <https://www.copergas.com.br/atendimento-ao-cliente/tarifas/>.

Dudley, V. E., Kolb, G. J., Sloan, M. and Kearney, D. “Test results: SEGS LS-2 solar collector”. SAND94-1884, Albuquerque, NM; 1994.

Fernández-García, A., Zarza, E., Valenzuela, L., Pérez, M. “Parabolic-trough solar collectors and their applications”. Renewable and Sustainable Energy Reviews, Vol. 14, n. 7, p. 1695–1721, 2010.

Gorenflo D.; Kenning D. *H2 Pool Boiling. VDI Heat Atlas*. p. 757–792, 2009. Springer, Berlin, 2010.

Häberle, A. “Concentrating solar technologies for industrial process heat and cooling”. *Concentrating Solar Power Technology*, p. 602–619, 2012.

Kalogirou, S, 2014. *Solar energy engineering: processes and systems*, Elsevier Academic Press, Amsterdam.

Kalogirou, S. A. “A detailed thermal model of a parabolic trough collector receiver”. Energy, Vol. 48, n. 1, p. 298–306, 2012.

Kind, M.; Saito, Y. *VDI heat atlas.* Springer, Berlin, 2010.

Kurup, P and Turchi, C. “Initial Investigation into the Potential of CSP Industrial Process Heat for the Southwest United States”. Jan. 2015.

Kutscher, C. F., Davenport, R. L., Dougherty, D. A., Gee, R. C., Masterson, P. M. and May, E. K. “Design approaches for solar industrial process heat systems: Nontracking and Line-Focus Collector Technologies*”.* Bascom, OH: Solar Energy Information Services (SEIS), 1983.

Murphy, L. M. and May, E. K. “Steam generation in line-focus solar collectors*: a comparative assessment of thermal performance, operating stability, and cost issues”* Golden, CO: Solar Energy Research Institute, 1982.

NATURAL RESOURCES CANADA. “Natural Gas Facts". 27 mar. 2018. <https://www.nrcan.gc.ca/energy/facts/natural-gas/20067#L1>.

NREL. ”National Solar Radiation Data Base”. 05 dez. 2017. <https://nsrdb.nrel.gov/nsrdb-viewer>

Powell, K. M.; Edgar, T. F. “Modeling and control of a solar thermal power plant with thermal energy storage”. *Chemical Engineering Science*, Vol. 71, p. 138–145, 2012.

Powell, K. M.; Hedengren, J. D.; Edgar, T. F. “Dynamic optimization of a hybrid solar thermal and fossil fuel system”. *Solar Energy*, Vol. 108, p. 210–218, 2014.

RACKAM, 2018. “Catálogo: S10 Parabolic Trough System “. 15 Jan. 2018. <https://rackam.com/en/products/s10/>.

Sharma, A. K.; Sharma, C.; Mullick, S. C.; Kandpal, T. C. *“Solar Industrial process heating: A review”*. *Renewable and Sustainable Energy Reviews*, Vol. 78, p. 124-137, 2017.

Thome, J. R.; Hajal, J. E. “Two-Phase Flow Pattern Map for Evaporation in Horizontal Tubes: Latest Version”. *Heat Transfer Engineering*, Vol. 24, n. 6, p. 3–10, 2003.

Xiao, X.; Yin, H. “Achieving higher order of convergence for solving systems of nonlinear equations”. *Applied Mathematics and Computation*, Vol. 311, p. 251–261, 2017.

7. RESPONSIBILITY NOTICE

The authors are the only responsible for the printed material included in this paper.